ELSEVIER

PII: S0032-3861(97)10333-0

Polymer Vol. 39 No. 17, pp. 4037–4045, 1998

0032-3861/98/$19.00+0.00

Effect of intramolecular reaction on the properties of polybutadiene–silane rubbers

María S. Di Nezio, Claudia Sarmoria and Enrique M. Vallés*
Planta Piloto de Ingeniería Química, UNS-CONICET, 12 de octubre 1842, (8000) Bahía Blanca, Argentina
(Received 24 January 1997; revised 23 June 1997; accepted 25 November 1997)

Model networks were prepared by the reaction of monodisperse polybutadiene, containing 8% of double bonds in the 1,2 vinyl position, with p-bis(dimethyl silyl) benzene at different stoichiometric imbalances. Small strain modulus and measurements of the gel fraction indicate important differences with the predictions from ideal network forming reactions and the molecular theories of rubberlike elasticity. Sol extractions are higher than expected and small strain moduli are consistently low. Other macroscopic signs of the departure from ideal behaviour are detected. The onset of the gel point is delayed to a degree that grows with increasing imbalance of the reactive groups. We consider all the possible explanations for the observed behaviour, and suggest that the most likely one is the presence of intramolecular reaction. We also propose a simple theoretical model to confirm that our assumptions are consistent with the experimental results. © 1998 Elsevier Science Ltd. All rights reserved.

(Keywords: intramolecular reaction; polybutadiene–silane rubbers; model networks)

INTRODUCTION

Different theories have been proposed to relate the molecular structure of rubber networks to their elastic properties. One of the major controversies in this respect is that concerning the contribution of molecular entanglements. The phantom network model considers a network composed of a collection of Gaussian random chains whose conformations are independent of neighbouring chains. In this idealized behaviour the junctions at which the chain ends are connected can fluctuate freely, that is, all chains may adopt any conformation. This 'phantom chain' formulation gives, for the shear modulus G, the following result[1,2]:

$$G = (\nu - \mu)RT \tag{1}$$

where ν and μ are the concentrations of elastically active chains and junctions, respectively, R is the universal gas constant and T is the absolute temperature. In this model the effect of entanglements resulting from the excluded volume due to chain-to-chain interactions is not taken into consideration.

Revisions of the phantom theory to take the effect of entanglements into account form the basis of various current molecular theories of rubber elasticity. The so called 'affine deformation' model[3–7] assumes that the deviation of real networks from phantom networks results from restrictions affecting the mobility of the chain junctions. From this point of view the constraints imposed by the presence of entanglements alter the independent fluctuation of the junctions making them move in a fashion that is affine with the macroscopic deformation of the network. Under this supposition the following expression is obtained:

$$G = \nu RT \tag{2}$$

Other research groups consider that chains contribute to the mechanical properties not only through their junction points, but also through contacts along their contour. This is based on the experimental observation of a rubbery plateau modulus, G_N^0, for linear polymers of high molecular weight, something that indicates that chain-chain interactions must be present in uncrosslinked samples. Some of those interactions could conceivably become trapped as crosslinks are introduced into the system, and these trapped entanglements would contribute to the shear modulus. Based on these arguments Langley[8] and Graessley[9,10] proposed that

$$G = (\nu - h\mu)RT + G_e T_e \tag{3}$$

where G_e is the 'entanglement modulus', close to G_N^0, T_e is the entanglement trapping factor, and h is a factor that may vary between 0 and 1. Equation (3) is the most general because it contains equations (1) and (2) as special cases. We see from equation (3) that in order to get the phantom chain formulation $G_e T_e$ must be zero. It has been shown that this is very unlikely[5–7]. The phantom chain formulation, then, is a lower bound on the admissible values of shear modulus.

The initial goal of this work was to investigate the contribution of entanglements with a well-defined experimental system. The crosslinking of polybutadienes (PB) of narrow molecular weight distributions was chosen because this polymer has a high plateau modulus. It was expected that this property would be helpful in evaluating the term that accounts for trapped entanglements in equation (3). The pendant vinyl groups from the PB were crosslinked with a bifunctional silane using the hydrosilation reaction. Different networks were obtained using a range of stoichiometric imbalances. They went from values around unity—which implies perfect crosslinking of all vinyl groups—to the so called 'critical imbalance', beyond which gelation is impossible. The resulting networks exhibited higher soluble

* To whom correspondence should be addressed

fractions than expected and consistently low equilibrium moduli. Since both gel fractions and elastic moduli were reproducible, and the absence of side reactions was confirmed, this particular behaviour is attributed to the presence of intramolecular reactions in the curing process. A simple theoretical model was developed to confirm that our assumptions were consistent with the observed behaviour. The results are in very good agreement with the experiments. Unfortunately, as the concentration of trapped entanglements obtained in the presence of intramolecular reactions is low, no valid conclusions were obtained with respect to the capability of the trapped entanglement term in equation (3) to give a better fit of the experimental elastic modulus measurements.

EXPERIMENTAL

Linear polybutadienes with narrow molecular weight distributions were synthesized in our laboratory by anionic polymerization. Polybutadienes of two molecular weights were used in this work: the first one had an $M_n = 8200$ and a polydispersity (PD) of 1.03, measured by g.p.c., while the second one had an $M_n = 12\,200$ and a PD = 1.04. They are identified in this work as PB82 and PB122 as indicated in *Table 1*. Vapour-phase osmometry (VPO) was used to confirm the g.p.c. results. Values of M_n obtained by this method were 8450 for polymer PB82 and 12 700 for polymer PB122. It has been shown that the polybutadiene chains obtained by anionic polymerization contain randomly distributed double bonds in the *cis*, *trans* and 1,2 vinyl positions[11]. The overall proportion of vinyl groups is determined by reaction conditions[12–14]. Polybutadienes used in this work had 8% of double bonds in the 1,2 vinyl position as determined by infrared spectroscopy in a Nicolet 520 *FT*i.r. instrument. The peak at 910 cm^{-1} was used for this purpose.

The crosslinker was a disilane reactant, p-bis(dimethyl silyl) benzene, purchased from Petrarch Systems. Its purity was 98% as indicated by gas chromatography. It was used without further purification.

The vinyl-silane hydrosilation reaction was catalyzed using a platinum salt: Pt $Cl_2(S(CH_2CH_3)_2)_2$. In order to achieve reasonable curing times, reactions were carried out at 60°C with a platinum concentration of 400 ppm. Under these conditions the networks cured in less than 24 h. It was verified that polybutadiene did not degrade at that temperature by preparing two mixtures of polybutadiene and catalyst without crosslinker and heating them under different conditions. One sample was heated for 7 h at 70°C in air, and the other one was subjected to the same treatment under nitrogen. A third sample of unheated pure polybutadiene was analysed as a reference. Infrared and gel permeation chromatography studies on all three samples showed no significant differences between them, indicating that no degradation had occurred.

Since the vinyl groups are the only ones in this system that may react with the crosslinker, the number of vinyl groups on any given chain equals its functionality. Therefore, the polybutadiene chains used in this work were practically monodisperse in mass but polydisperse in functionality.

Networks were obtained using a range of stoichiometric imbalances, r, where r is defined as the ratio of moles of vinyl groups to moles of silane groups. As secondary reactions are known to affect the hydrosilation curing when vinyl groups are in defect[15], the majority of imbalanced reactions were run with an excess of vinyl groups to avoid that condition.

Two properties were measured on the completely cured samples: gel fraction and elastic modulus. In order to measure gel fraction, the soluble part of each network sample was extracted. Two different techniques were used. Some samples were extracted using a standard Soxhlet apparatus with cellulose thimbles and normal hexane as a solvent. Since the thimbles readily absorbed air humidity, their weight changed with time after removal from the oven, introducing some error in the measurements (specially at low gel fractions). For this reason the cellulose thimbles were washed in hexane and dried before use, and time–weight curves were established for each empty thimble. That procedure made it possible to extrapolate the measured weight to zero time, when no air humidity had been absorbed. This procedure proved to be very reliable. Low gel fractions could be measured reproducibly. Other samples were extracted using closed jars where the solvent was periodically renewed. Both procedures yielded comparable results. Gel fraction data for networks prepared from both prepolymers are shown in *Table 2*.

Elastic modulus was measured on completely cured samples using a Rheometrics Mechanical Spectrometer. Dynamic moduli were measured using parallel-plate geometry. Measurements were carried out at 60°C under a nitrogen atmosphere. It is well known[16] that $G'(\omega)$ is related to the time-dependent equilibrium relaxation shear modulus $G(t)$, since both are a measure of the stored elastic energy in the tested material. Furthermore, the constant value of $G'(\omega)$ that is characteristic of low frequencies is equivalent to the constant equilibrium shear modulus characteristic of long relaxation times, G_e. In the samples studied, $G'(\omega)$ was constant (within experimental error) for the range of frequencies between 0.1 and 100 rad/s. Therefore, those measured values were taken as equal to G_e. Since we will not use any other modulus, we will just denote it as G in the remainder of the paper. The measurements were performed on samples that had not been extracted. Elastic data are shown in *Table 3*.

RESULTS AND DISCUSSION

The results from the sol extractions on the different networks in *Table 2* were compared with the calculations for the gel fraction obtained by the classical recursive approach introduced by Miller and Macosko[17–20]. The calculations were based on the general assumptions for ideal

Table 1 Characterization of the linear polybutadienes

Polymer identification	g.p.c.			Vapor phase osmometry	Double bonds (%)		
	M_n	M_w	PD	M_n	*trans*	*cis*	vinyl
PB82	8200	8450	1.03	8650	49.5	42.6	7.9
PB122	12 200	12 700	1.04	12 500	45.5	46.5	8.0

network-forming polymerizations, i.e. the accessibility to reaction of each reactive site in the molecules is independent of its position in the chain, all the chains are equally reactive, there are no substitution effects and no intramolecular reactions[21]. These results show that the agreement between theoretical and experimental values for PB82 samples is reasonably good for imbalances up to about two. For larger imbalances, however, the ideal predictions for gel fraction are consistently larger than the measured values for both polymers. The magnitude of the differences becomes unacceptably high for values of $r > 3$. Here, all ideal predictions overestimate the measured gel fraction. These results cannot be attributed to experimental errors since they have been checked several times. Therefore some kind of departure from the ideal crosslinking process has to be explored. The two more probable sources of non-ideal behaviour in this system are the presence of secondary reactions or the occurrence of intramolecular reactions taking place between the crosslinker and the different vinyl groups that belong to the same polybutadiene molecule. Both problems result in the consumption of some of the chemical groups that would otherwise remain available for the crosslinking reaction, thus reducing the amount of gel and lowering the elastic properties of the network.

Measurements of the elastic modulus from the different networks synthesized from polymers PB82 and PB122 are shown in *Table 3*. The experimental results are compared with those predicted from the phantom network theory (equation (1)) where ν was again calculated with the recursive approach for ideal polymerization. Here again, as in the gel fraction measurements, the results show a departure from the predicted values. The deviations with polymer PB82 become more important at values of $r > 3$ while they are not as evident with polymer PB122. It is important to note that the maximum in elastic modulus appears for networks synthesized at an imbalance of unity.

Table 2 Experimental and theoretical values of the gel fraction for different networks synthesized from polybutadiene prepolymers

Sample	r = [Vi]/[Si]	Gel fraction		
		Experimental	Calculated ideal network without intramolecular reactions	Calculated network with intramolecular reactions
PB82-1	0.70	1.000	0.985	0.962
PB82-2	1.00	1.000	0.999	0.990
PB82-3	1.07	1.000	0.999	0.990
PB82-4	1.48	1.000	0.999	0.984
PB82-5	1.82	1.000	0.999	0.969
PB82-6	2.08	1.000	0.997	0.952
PB82-7	2.16	0.795	0.996	0.946
PB82-8	2.77	0.881	0.988	0.884
PB82-9	2.98	0.882	0.982	0.857
PB82-10	3.45	0.656	0.968	0.785
PB82-11	3.70	0.728	0.958	0.744
PB82-12	4.65	0.591	0.907	0.552
PB82-13	4.83	0.572	0.895	0.511
PB82-14	4.97	0.512	0.885	0.479
PB82-15	7.70	0.031	0.622	0.000
PB82-16	7.89	0.030	0.599	0.000
PB82-17	8.46	0.021	0.527	0.000
PB82-18	9.12	0.019	0.438	0.000
PB122-1	7.10	0.457	0.898	0.533
PB122-2	7.80	0.438	0.864	0.422
PB122-3	11.3	0.000	0.634	0.000
PB122-4	11.7	0.000	0.601	0.000
PB122-5	12.1	0.000	0.568	0.000
PB122-6	12.7	0.000	0.517	0.000
PB122-7	13.8	0.000	0.417	0.000

Table 3 Experimental and theoretical values of the elastic modulus for different networks

PB type	r	$G \times 10^{-6}$ (Pa) experim.	$G \times 10^{-6}$ (Pa) phantom (equation (1))		$G \times 10^{-6}$ (Pa) affine (equation (2))		$G \times 10^{-6}$ (Pa) Langley (equation (3))	
			Ideal	Intram. reaction	Ideal	Intram. reaction	Ideal	Intram. reaction
PB82	0.95	1.250	1.378	0.638	2.999	1.478	2.988	1.555
PB82	0.99	1.050	1.456	0.663	3.159	1.529	3.131	1.604
PB82	1.00	1.470	1.476	0.668	3.199	1.541	3.167	1.616
PB82	1.08	1.430	1.357	0.606	2.960	1.411	2.948	1.485
PB82	1.48	0.920	0.939	0.386	2.110	0.937	2.154	0.994
PB82	2.02	0.540	0.620	0.219	1.448	0.557	1.508	0.588
PB82	3.02	0.187	0.322	0.077	0.798	0.208	0.840	0.213
PB82	4.09	0.060	0.169	0.017	0.439	0.049	0.459	0.047
PB82	4.83	0.012	0.109	0.007	0.289	0.020	0.298	0.018
PB122	0.90	1.330	1.394	0.704	2.962	1.562	3.029	1.733
PB122	0.99	1.380	1.574	0.762	3.324	1.601	3.350	1.845
PB122	1.03	1.620	1.547	0.743	3.271	1.644	3.303	1.809
PB122	1.10	1.260	1.447	0.692	3.071	1.540	3.123	1.706
PB122	1.29	1.190	1.225	0.576	2.626	1.303	2.719	1.466
PB122	2.15	0.745	0.680	0.285	1.523	0.687	1.676	0.801

This is a result consistent with the absence of secondary reactions. If one of the chemical groups participating in the reaction were consumed in one or more secondary reactions, the addition of this reactant in excess to the stoichiometric amount would compensate for the wasted groups, resulting in a perfect network with maximum modulus at an imbalance other than unity. To further explore the possible presence of secondary reactions the concentration of silane and vinyl groups was simultaneously followed by *FT*i.r. in several reacting systems as a function of time. The 4725 cm^{-1} vinyl peak and the 2121 cm^{-1} silane peak were used for this purpose. The results, as shown in *Figure 1*, indicated that the rate of consumption of silane and vinyl groups was the same in every case. This is also consistent with the absence of secondary reactions.

Since both gel fraction and elastic modulus measurements were reproducible, and side reactions did not seem to be present, another explanation must be given for the reported differences in the gel fractions and the experimental values of G. One possibility would be the presence of intramolecular reaction in the curing process. The high functionality of the polybutadiene chains would tend to favour intramolecular reaction. If it did occur, it would consume reactive sites without adding mass to the growing molecules or elastically active chains to the network. The gel point would be delayed, the gel fraction and the elastic modulus at any given imbalance would be lower than expected, as was detected in our experiments. In order to confirm that intramolecular reactions could indeed be the explanation for the observed behaviour, we have implemented a simple model that takes these reactions into account. We have modelled this system using the Spanning Tree approximation[22]. This is a two-step formalism. In the first step, kinetic differential equations must be solved in order to calculate the concentration of the conceptual building blocks of the network. The building blocks are defined in such a way as to distinguish between unreacted, intermolecularly reacted, or intramolecularly reacted sites. Using the standard notation of the Spanning Tree approximation[22], sites that are unreacted are referred to as ω-sites, those that have reacted intermolecularly as α-sites, and the ones that have reacted intramolecularly as σ-sites. In the second step, these building blocks are combined at random to give statistical trees[23] that represent the molecules in the reacted system. The blocks are joined by the intermolecularly reacted sites only. As a result, the intramolecularly reacted sites act as dead ends and are randomly distributed throughout the tree. This model allows one to compute the total number of intramolecularly reacted sites, but keeps no information on the size of the rings formed[23]. We have chosen this model because it is a simple one that requires very few equations. It is appropriate for our aim of confirming that the presence of intramolecular reactions is consistent with the observed behaviour of the experimental system. The details of the derivation are explained in Appendix A.

The proposed model has one adjustable parameter, D, which is used to evaluate the correct ring-closing concentration. This model, like all others proposed for treating systems with intramolecular reaction, needs to evaluate the concentration of potentially ring-closing sites around a given unreacted site. Historically, a Gaussian end-to-end distance distribution has been assumed[22,24–26]. For two sites that are j units apart, this concentration is

$$C_j = \left(\frac{1.5}{j\pi n_b}\right)^{1.5} \frac{1}{l^3 N_A} \tag{4}$$

where n_b is the number of bonds contributed by each of the j units, l is the bond length and N_A is Avogadro's number. Since real chains are more extended than the Gaussian distribution indicates[27], some adjusting factor is necessary to correct the concentration. Some authors have chosen to use a different rate constant for intermolecular and intramolecular reaction[22]. This is equivalent to using the same rate constant for every reaction and multiplying C_j above by an adjustment factor. Others replace the physical bond length l by an 'effective bond length[24], which could be assimilated

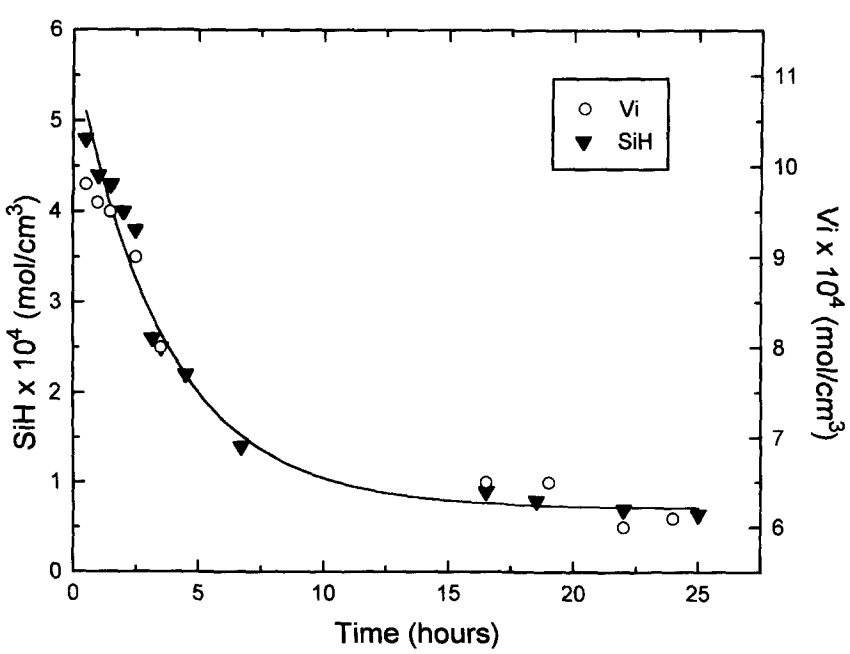

Figure 1 Concentration of vinyl and silane groups at different times during a stoichiometrically imbalanced curing reaction, as calculated from i.r. measurements. The Y-axes have been displaced to show that the rate of consumption of both reactive groups is the same. The full line is an exponential fit through the data

to dividing C_j by an adjustment parameter. In this work we have chosen to use the same rate constant for all reactions, and the physical bond length, and correct the concentration C_j by dividing it by an adjustable parameter D. Its value was determined using experimental data for the weight fraction of gel from the different rubbers synthesized with polymer PB82. We show in *Figure 2* the experimental values of gel fraction at complete reaction *versus* the inverse of the stoichiometric imbalance, $1/r$. We also show in the same figure the predictions for the gel fraction that were obtained using the proposed model with different values of D. The ideal curve that corresponds to a reaction system without intramolecular reactions is obtained with an infinite value of D. We can see that it consistently overestimates the gel fraction. On the other hand, the curve with $D = 1$, corresponding to a perfect Gaussian end-to-end distance distribution of the chain ends, consistently underestimates that value. The third curve on the plot is for $D = 4.5$, the curve that provides the best fit to the experimental data. That is the value of D that was used in the remainder of the work.

With a fixed value of D already established from the comparison with the sol extraction experiments from polymer PB82, we calculated the gel fraction for polymer PB122 and found very good agreement with the experimental gel fractions as shown in *Table 2*. The same value of the parameter D was used to compute the fraction of σ-sites as a function of extent of reaction for different stoichiometric imbalances r. In *Figure 3* we plot the results of such a calculation for networks synthesized from PB82. We see that for completely cured samples the maximum number fraction of intramolecularly reacted sites occurs at $r = 1$. This happens because the maximum extent of reaction is higher at $r = 1$. If we were to compare samples at the same extent of reaction, then the networks with higher stoichiometric imbalances contain more σ-sites than the ones with lower imbalances.

After this we calculated the elastic parameters of the networks, that is, the concentration of elastically active chains and junctions. Those quantities were used to calculate the elastic modulus G according to the three formulations of the theory of rubber elasticity described in the introduction: the 'phantom chain', the 'affine deformation' and the Langley and Graessley model. Values of G were calculated for those formulations with and without rings allowed. The calculated moduli were compared with experimental data obtained with networks synthesized from PB82 in experiments that were independent of those used to adjust the value of D. The results of the comparison are shown in *Figure 4*. We can see that the agreement between theory and experiment is better when rings are allowed for in the curing reaction. The results of a similar comparison with the measurements performed on networks synthesized from PB122 are shown in *Table 3*. We see that there is good agreement between the predictions from equation (2) equation (3) and the experimental measurements when intramolecular reactions are taken into account. Networks with stoichiometric imbalances in the vicinity of $r = 1$ showed the greatest deviation from ideal behaviour. This is not evident from the semi-logarithmic plots of *Figure 4*, but absolute differences in modulus between expected values of G with and without intramolecular reactions are considerably higher at balanced stoichiometries as shown in columns 6–9 of *Table 3*. This is in accordance with the theoretical results in *Figure 3* that indicate the maximal concentration of intramolecular reactions, and therefore the highest amount of lost sites available for crosslinking, in the region around $r = 1$.

Unfortunately as the amount of trapped entanglements calculated with the reported levels of intramolecular reactions is not important, either equation (2) or equation (3) can fit the experimental results for G with the same degree of accuracy. This is shown in *Figure 4* where equation (3) was used with a value of $G_N^0 = 0.7$ mPa and $h = 0.3$, values that were obtained by least squares fitting of the experimental data. The value of G_N^0 is in good agreement with previously reported values for similar systems (0.7–0.96 mPa)[15]. Therefore this set of experiments was not useful to assess the way in which the restrictions to chain mobility affect the elastic properties of a rubber network. A

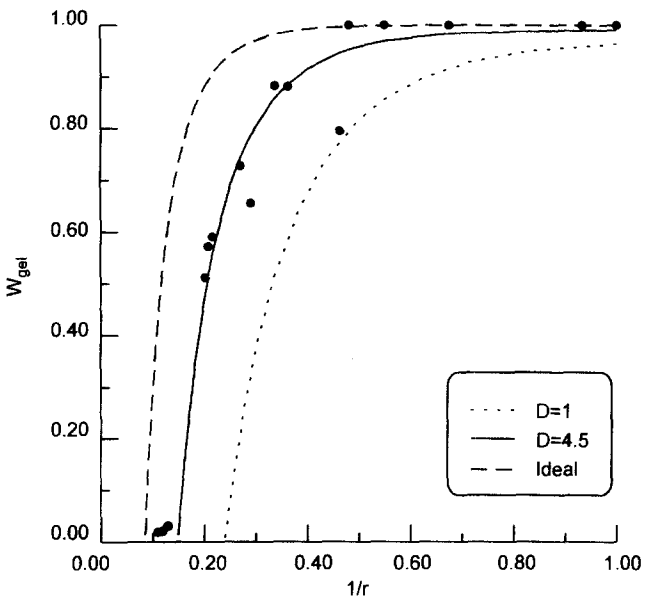

Figure 2 Weight fraction of gel at complete reaction *versus* the inverse of the stoichiometric imbalance for polybutadiene of molecular weight $M_W = 8200$. The filled circles represent experimental data. The different lines indicate the predictions using different values of the adjustable parameter D

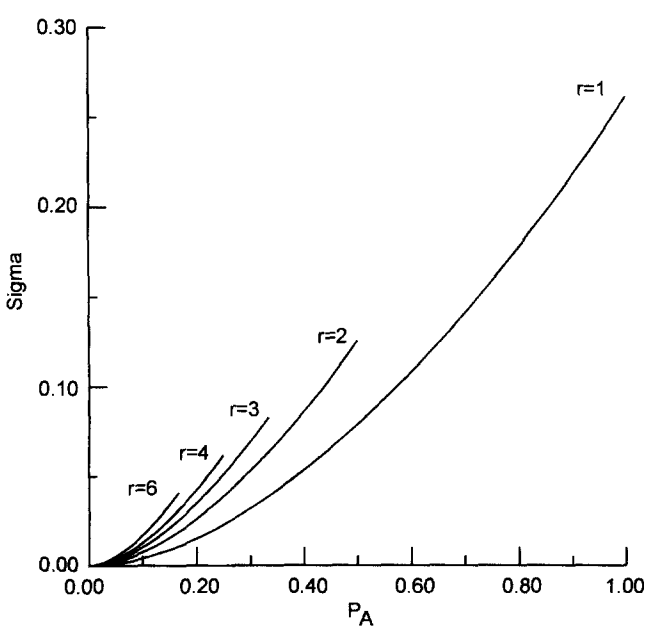

Figure 3 Number fraction of intramolecularly reacted sites for different networks synthesized from polybutadiene of molecular weight 8200. Curves are interrupted at the maximum attainable extent of reaction. The stoichiometric imbalance used is indicated on each curve

new system based on the crosslinking of PB chains with reactive groups on the extremes of the chains may be more appropriate for the study of this problem.

CONCLUSIONS

We have found that networks prepared by reaction of monodisperse polybutadienes with bi-functional disilanes do not behave as expected for a regular crosslinking process in which intramolecular reactions are not important. Sol fractions are higher than expected, small strain moduli are consistently low, and the onset of the gel point is delayed to a degree that grows with increasing imbalance of the reactive groups. The experimental results from sol fraction and elastic modulus measurements are consistent with the predictions of a mathematical model which takes into account the presence of intramolecular reactions. This same qualitative behaviour has been reported by other authors[28,29] on several endlinking systems synthesized at different degrees of dilution, where it was attributed to the presence of intramolecular reaction.

The mathematical model that was developed for this work has the advantage of being very simple and requiring only one adjustable parameter D. It gives as a result the concentration of sites reacted intramolecularly but does not provide important information such as the sizes of rings involved. The results indicate that, indeed, intramolecular reaction could explain the observed anomalous behavior of the synthesized networks.

ACKNOWLEDGEMENTS

This research work was supported by CONICET, the National Research Council of Argentina, and by Universidad Nacional del Sur.

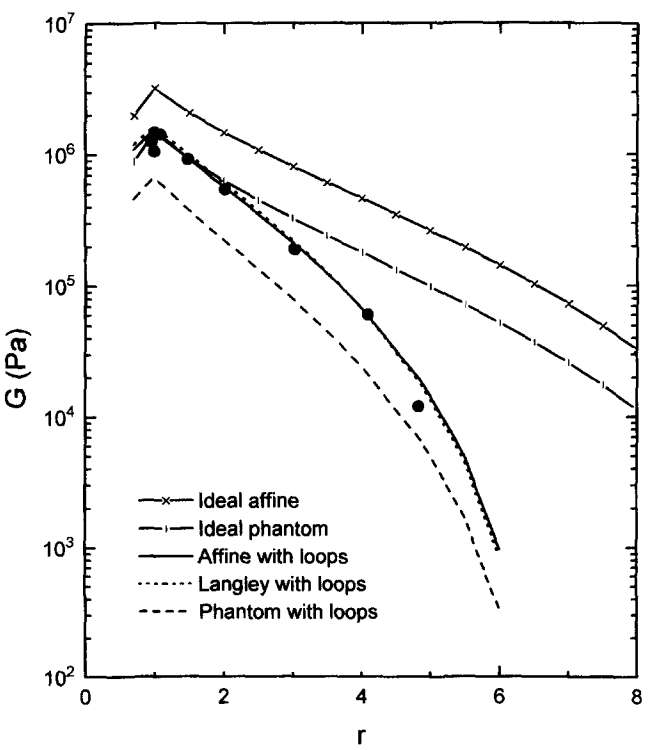

Figure 4 Elastic modulus G *versus* the stoichiometric imbalance for polybutadiene of molecular weight $M_W = 8200$. The filled circles represent experimental data. The predictions of different theories with and without loops are indicated with different lines

APPENDIX A:

We have modelled the crosslinking reaction using the Spanning Tree approximation[22]. The building blocks used for modelling the polybutadiene–silane system are shown in *Figure 5*. The A-structures make up the polybutadiene chains. The A_1 structure represents a repeat unit without a reactive site, that is, a butadiene unit with a double bond in either the *cis* or the *trans* position. The remaining A-structures represent repeat units with reactive sites: butadiene units that added double bonds in the 1,2 vinyl position to the chain. Using the standard notation of the Spanning Tree approximation[22], sites that are unreacted are referred to as ω-sites, those that reacted intermolecularly as α-sites, and the ones that reacted intramolecularly as σ-sites. A_2 is the repeat unit with an ω (unreacted) vinyl, A_3 is the repeat unit with an α vinyl, and A_4 is the repeat unit with a σ vinyl. It is known in advance that a proportion p of all repeat units have reactive sites. Any chain is made up of exactly m randomly chosen A-structures, m being the degree of polymerization of the original (uncrosslinked) polybutadiene chains. This reflects the fact that the polybutadiene chains are monodisperse in length but polydisperse in functionality. The average functionality of the chains is $F = mp$. This is both a number and a weight average, since all m repeat units weigh the same.

The B-structures in *Figure 5* represent disilane molecules in different states: B_1 is the unreacted disilane, B_2 is a disilane with one reacted site, B_3 is a disilane with two intermolecularly reacted sites, and B_4 is a disilane with one intermolecularly reacted site and one intramolecularly reacted site. Notice that the reacted site in B_2 is labelled as an α-site, since a unit with two reactive sites must react intermolecularly before it can do so intramolecularly.

If the concentrations of all the structures in *Figure 5* are known, they may be used to construct statistical trees that represent the molecules in the reacting system. One such tree is shown in *Figure 6*. For the purpose of illustration, dotted lines indicate possible intramolecular bonds. In practice, however, it is impossible to know which A_4 unit is connected to which B_4 unit because this information is not saved. Notice also that since units are joined at random, nothing prevents the presence of an uneven number of σ-sites in the molecule.

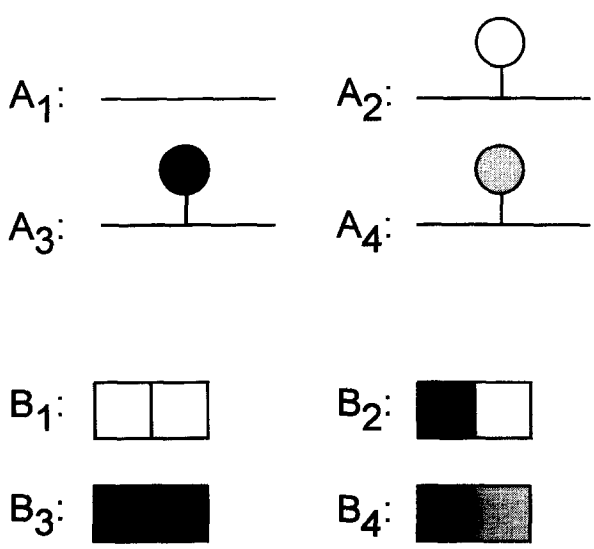

Figure 5 Building blocks necessary to describe the polybutadiene–silane copolymerization. White areas are unreacted sites; black areas are intermolecularly reacted sites; grey areas are intramolecularly reacted sites

The one in *Figure 6*, for example, contains three A^{σ} and two B^{σ} sites.

The concentrations of the differently labelled sites may be easily found from the concentrations of the structures in *Figure 5*. Let $A_i(t)$ stand for the concentration of structure A_i at time t, $B_i(t)$ stand for the concentration of structure B_i at time t, $A^{\sigma}(t)$ represents the concentration of A-sites labelled σ at time t, and $B^{\sigma}(t)$ the concentration of B-sites labelled σ at time t. Then

$$A^{\omega}(t) = A_2(t) \tag{A1}$$

$$A^{\alpha}(t) = A_3(t)$$

$$A^{\sigma}(t) = A_4(t)$$

$$B^{\omega}(t) = 2B_1(t) + B_2(t)$$

$$B^{\alpha}(t) = B_2(t) + 2B_3(t) + B_4(t)$$

$$B^{\sigma}(t) = B_4(t)$$

In order to find out the concentration of each of the structures in *Figure 5*, a system of kinetic differential equations is set up. If k is the rate constant, the equations may be expressed as

$$\frac{dA_1(t)}{dt} = 0 \tag{A2}$$

$$\frac{dA_2(t)}{dt} = -kA_2(t)B^{\omega}(t) - kA_2(t)B^{*}(t)$$

$$\frac{dA_3(t)}{dt} = kA_2(t)B^{\omega}(t)$$

$$\frac{dA_4(t)}{dt} = kA_2(t)B^{*}(t)$$

$$\frac{dB_1(t)}{dt} = -2kB_1(t)A^{\omega}(t)$$

$$\frac{dB_2(t)}{dt} = 2kB_1(t)A^{\omega}(t) - kB_2(t)A^{\omega}(t) - kB_2(t)A^{*}(t)$$

$$\frac{dB_3(t)}{dt} = kB_2(t)A^{\omega}(t)$$

$$\frac{dB_4(t)}{dt} = kB_2(t)A^{*}(t)$$

where $A^{*}(t)$ and $B^{*}(t)$ are ring-closing concentrations that are calculated as follows. Given an unreacted B-site, $A^{*}(t)$ is the concentration of potentially ring-closing A-sites in the vicinity of that B-site. In order to have the potential to close a ring with the B-site, the A-sites in question must be on the same molecule. So in order to evaluate $A^{*}(t)$ it is necessary to count the unreacted A-sites that belong to the same molecule as the B-site. Counting them up, however, is not enough. A-sites that are far away from the given B-site will be less likely to react with it than A-sites that are close by. The evaluation of a concentration requires the number of A-sites to be weighted by a function that will take this fact into account. Historically, a Gaussian end-to-end distance distribution has been used for this purpose[22,24–26]. Since real chains are more extended than the Gaussian distribution indicates[27], in this paper we divide the resulting concentration by an arbitrary constant D that is used as an adjustable parameter. $A^{*}(t)$ and $B^{*}(t)$ are found in analogous ways. For the purposes of illustration, we will only show the derivation of $B^{*}(t)$.

Given that an A^{ω} and a B^{ω} site are j units apart, that all units contribute n_b bonds to the chain, and assuming a Gaussian end-to-end distance distribution, the concentration of those two ω sites around each other is

$$C_j = \frac{\xi}{(jn_b)^{1.5}} \tag{A3}$$

where $\xi = (1.5/\pi)^{1.5}\,(l/l^3N_A)$, l is the bond length, and N_A is Avogadro's number.

In order to calculate $B^{*}(t)$, we pick an unreacted A-site at random. This is equivalent to randomly picking an A_2 structure. In our model, the A-structures are distributed at random among the chains, subject to the constraint that each chain contains exactly m A-structures. Therefore, the chance that the randomly chosen A_2 will be on any given position along the polybutadiene chain is $1/m$. Then,

$$B^{*}(t) = \sum_{i=1}^{m} \frac{1}{m} B_i^{*}(t) \tag{A4}$$

where $B_i^{*}(t)$ is the ring closing concentration of B^{ω} on the same chain given that the randomly chosen A_2 is on the ith position along the chain. Now we evaluate each of the $B_i^{*}(t)$. In *Figure 6*, for example, the A_2 structure marked with a star was chosen. This A^{ω} site may react intramolecularly with any of the two B^{ω} sites that appear in the figure. Starting from the chosen A_2 structure, we must move along the chain one monomer unit at a time. At any given position along a chain we may find one of the A_i structures with probabilities

$$P(A_1) = 1 - p \tag{A5}$$

$$P(A_2) = p\frac{A_2(t)}{A_2(t) + A_3(t) + A_4(t)}$$

$$P(A_3) = p\frac{A_3(t)}{A_2(t) + A_3(t) + A_4(t)}$$

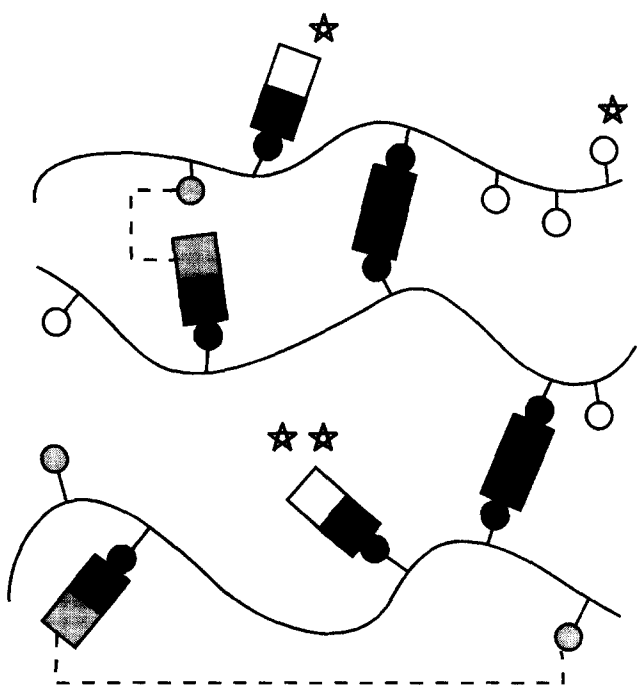

Figure 6 sample molecule constructed from the building blocks of *Figure 5*. All chains contain the same number of monomers

$$P(A_4)=p\frac{A_4(t)}{A_2(t)+A_3(t)+A_4(t)}$$

These probabilities are the same for all positions along the chain, since the distribution is random. We are searching for unreacted B-sites that are already connected to the molecule. Those sites must be on B-structures, connected to the molecule through A_3 structures. Then, the probability of finding B_i given that we have an A_3 is

$$P(B_1|A_3)=0 \tag{A6}$$

$$P(B_2|A_3)=\frac{B_2}{B_2+2B_3+B_4}$$

$$P(B_3|A_3)=\frac{2B_3}{B_2+2B_3+B_4}$$

$$P(B_4|A_3)=\frac{B_4}{B_2+2B_3+B_4}$$

Now, let us suppose that the randomly chosen A_2 is on one end of a polybutadiene chain. Then, we must find $B_1^*(t)$.

$$B_1^*(t)=\sum_{j=1}^{m-1}\frac{\xi}{(jn_b)^{1.5}}P(A_3)P(B_2|A_3)+\sum_{j=1}^{m-1}B_j^{in}(t)P(A_3)P(B_3|A_3) \tag{A7}$$

The first summation finds the concentration of sites such as the B^ω site marked with a single star in *Figure 6*, where the B^ω site is directly connected to the same polybutadiene chain as the randomly chosen A_2. The second summation takes into account B^ω sites such as the one marked with a double star in *Figure 6*. The site is on the same molecule, but on a different polybutadiene chain than the randomly chosen A_2. The connection is done through A_3's reacting with B_3's. $B_j^{in}(t)$ is the concentration around the chosen A_2 unit of B^ω sites that are on different chains and whose connection to the previous chain is j units away from the chosen A_2 unit. This distance must be taken into account for the evaluation of $B_j^{in}(t)$. This evaluation is shown later in Appendix A.

If the chosen A_2 site is on the second position along a chain, then when evaluating concentrations it is necessary to look in two directions, right and left from the chosen unit. With this in mind, we find that $B_2^*(t)$ should be

$$B_2^*(t)=\sum_{j=1}^{m-2}\frac{\xi}{(jn_b)^{1.5}}P(A_3)P(B_2|A_3)+\frac{\xi}{(n_b)^{1.5}}P(A_3)P(B_2|A_3)+\sum_{j=1}^{m-2}B_j^{in}(t)P(A_3)P(B_3|A_3)+B_1^{in}(t)P(A_3)P(B_3|A_3) \tag{A8}$$

If the chosen site is the third,

$$B_3^*(t)=\sum_{j=1}^{m-3}\frac{\xi}{(jn_b)^{1.5}}P(A_3)P(B_2|A_3)+\sum_{j=1}^{2}\frac{\xi}{(jn_b)^{1.5}}P(A_3)P(B_2|A_3)+\sum_{j=1}^{m-3}B_j^{in}(t)P(A_3)P(B_3|A_3)+\sum_{j=1}^{2}B_j^{in}(t)P(A_3)P(B_3|A_3) \tag{A9}$$

And, generally,

$$B_i^*(t)=\sum_{j=1}^{m-i}\frac{\xi}{(jn_b)^{1.5}}P(A_3)P(B_2|A_3)+\sum_{j=1}^{i-1}\frac{\xi}{(jn_b)^{1.5}}P(A_3)P(B_2|A_3)+\sum_{j=1}^{m-i}B_j^{in}(t)P(A_3)P(B_3|A_3)+\sum_{j=1}^{i-1}B_j^{in}(t)P(A_3)P(B_3|A_3) \tag{A10}$$

Substituting into equation (A4) gives

$$B^*(t)=\frac{1}{m}\sum_{i=1}^{m}\left[\sum_{j=1}^{m-i}\frac{\xi}{(jn_b)^{1.5}}P(A_3)P(B_2|A_3)+\sum_{j=1}^{i-1}\frac{\xi}{(jn_b)^{1.5}}P(A_3)P(B_2|A_3)\right]+\frac{1}{m}\sum_{i=1}^{m}\left[\sum_{j=1}^{m-i}B_j^{in}(t)P(A_3)P(B_3|A_3)+\sum_{j=1}^{i-1}B_j^{in}(t)P(A_3)P(B_3|A_3)\right] \tag{A11}$$

Substituting equations (A1), (A5) and (A6) into (A11), and dividing everything by the adjustable parameter D, we get.

$$B^*(t)=\frac{1}{mD}\sum_{i=1}^{m}p\frac{A_3(t)B_2(t)}{A^\omega(0)B^\alpha(t)}\left(\sum_{j=1}^{m-i}\frac{\xi}{(jn_b)^{1.5}}+\sum_{j=1}^{i-1}\frac{\xi}{(jn_b)^{1.5}}\right)+\frac{1}{mD}\sum_{i=1}^{m}p\frac{A_3(t)}{A^\omega(0)}\frac{2B_3(t)}{B^\alpha(t)}\left(\sum_{j=1}^{m-i}B_j^{in}(t)+\sum_{j=1}^{i-1}B_j^{in}(t)\right) \tag{A12}$$

The evaluation of $B_j^{in}(t)$ involves the same treatment that was required for $B^*(t)$. The only difference is that there are now (jn_b) extra bonds to be taken into account. The resulting equation is

$$B_j^{in}(t)=\frac{1}{m}\sum_{i=1}^{m}p\frac{A_3(t)B_2(t)}{A^\omega(0)B^\alpha(t)}\left(\sum_{n=1}^{m-i}\frac{\xi}{((j+n)n_b)^{1.5}}+\sum_{n=1}^{i-1}\frac{\xi}{((j+n)n_b)^{1.5}}\right)+\frac{1}{m}\sum_{i=1}^{m}p\frac{A_3(t)}{A^\omega(0)}\frac{2B_3(t)}{B^\alpha(t)}\times\left(\sum_{n=1}^{m-i}B_{j+n}^{in}(t)+\sum_{n=1}^{i-1}B_{j+n}^{in}(t)\right) \tag{A13}$$

Following a similar reasoning it is possible to find that

$$A^*(t)=\frac{1}{mD}\sum_{i=1}^{m}p\frac{A_3(t)}{A^\omega(0)}\left(\sum_{j=1}^{m-i}\frac{\xi}{(jn_b)^{1.5}}+\sum_{j=1}^{i-1}\frac{\xi}{(jn_b)^{1.5}}\right)+\frac{1}{mD}\sum_{i=1}^{m}p\frac{A_3(t)}{A^\omega(0)}\frac{2B_3(t)}{B^\alpha(t)}\left(\sum_{j=1}^{m-i}A_j^{in}(t)+\sum_{j=1}^{i-1}A_j^{in}(t)\right) \tag{A14}$$

where

$$A_j^{in}(t)=\frac{1}{m}\sum_{i=1}^{m}p\frac{A_2(t)}{A^\omega(0)}\left(\sum_{n=1}^{m-i}\frac{\xi}{((j+n)n_b)^{1.5}}+\sum_{n=1}^{i-1}\frac{\xi}{((j+n)n_b)^{1.5}}\right)+\frac{1}{m}\sum_{i=1}^{m}p\frac{A_3(t)}{A^\omega(0)}\frac{2B_3(t)}{B^\alpha(t)}\left(\sum_{n=1}^{m-i}A_{j+n}^{in}(t)+\sum_{n=1}^{i-1}A_{j+n}^{in}(t)\right) \tag{A15}$$

The differential equation for $A_1(t)$ indicates that this

concentration is constant. Its value is

$$A_1(t) = [\text{chains}]_0(m-F) = \frac{[\text{vinyl groups}]_0}{F}(m-F)$$
$$= [\text{vinyl groups}]_0\frac{(m-mp)}{mp} = [\text{vinyl groups}]_0\frac{(1-p)}{p} \quad \text{(A16)}$$

The set of seven remaining differential equations is solved numerically with initial conditions

$$A_2(0) = [\text{vinyl groups}]_0 \quad \text{(A17)}$$

$$A_i(0) = 0 \quad i = 3,\ 4$$

$$B_1(0) = [\text{disilane}]_0$$

$$B_i(0) = 0 \quad i = 2,\ 3,\ 4$$

At any time t the extent of reaction relative to A-sites is

$$P_A(t) = \frac{A_3(t)+A_4(t)}{A_2(t)+A_3(t)+A_4(t)} \quad \text{(A18)}$$

Once the concentrations of structures are known, they may be used to reconstruct the molecules at any given time t. The structures are put together at random under two constraints: the A-structures must make up chains containing exactly m units, and A^α and B^α sites are connected at random. A^σ and B^σ sites act as dead ends. In practice, this is equivalent to constructing an ideal statistical tree at an extent of reaction lower than the actual one, where only the intermolecularly reacted sites are taken into account. This 'intermolecular' extent of reaction could be defined as

$$P_{A\alpha}(t) = \frac{A_3(t)}{A_2(t)+A_3(t)+A_4(t)} \quad \text{(A19)}$$

We calculate the molecular parameters of the resulting statistical tree using the method proposed by Miller and Macosko for modelling the ideal crosslinking of chains with length and functionality distributions[19,20]. The one in this paper is a special case, where there is only functionality distribution. At any time t we use their method at the intermolecular extent of reaction $P_{A\alpha}(t)$.

$A^*(t)$ and $B^*(t)$ diverge beyond the gel point. This happens because just beyond the gel point there is one infinitely large molecule, and so the number of ω-sites that could close a ring with any given ω-site becomes infinite. The consequence is that the original Spanning Tree model may not be applied beyond the gel point. It has been proposed in the past to get around this problem by counting as σ-sites only those that close elastically inactive rings[26]. That is too complex for the purposes of this paper. Instead, we propose to truncate the summations in $A_j^{in}(t)$ and $B_j^{in}(t)$, so that an effective limit on the size of rings is attained. The largest allowed ring has as many bonds as 30 polybutadiene chains placed end by end. For the shortest polybutadiene used in this work, which has about 300 bonds, this is equivalent to a ring with over 9000 molecular bonds. We arrived at this value by allowing larger and larger rings until the results of the calculations showed no perceptible difference in the calculated elastic parameters. Elastic parameters were the most sensitive to the number of bonds allowed.

REFERENCES

1. James, H. M. and Guth, E., *J. Chem. Phys.*, 1947, **15**, 669.
2. Graessley, W. W., *Macromolecules*, 1975, **8**, 186.
3. Flory, P. J., *Proc. R. Soc. London, Sr. A*, 1976, **351**, 351.
4. Flory, P. J., *J. Chem. Phys.*, 1977, **66**, 5720.
5. Flory, P. J., *Polymer*, 1979, **20**, 1317.
6. Flory, P. J. and Erman, B., *Macromolecules*, 1982, **15**, 800.
7. Heinrich, G., Straube, E. and Helmis, G., *Adv. Polym. Sci.*, 1987, **84**, 33.
8. Langley, N. R., *Macromolecules*, 1968, **1**, 348.
9. Dossin, L. M. and Graessley, W. W., *Macromolecules*, 1979, **12**, 123.
10. Pearson, D. S. and Graessley, W. W., *Macromolecules*, 1980, **13**, 1001.
11. Carella, J. M., Graessley, W. W. and Fetters, L. J., *Macromolecules*, 1984, **17**, 2775.
12. Morton, M. and Fetters, L. J., *Rubber Chem. Technol.*, 1975, **48**, 359.
13. Hsieh, H. L., *J. Polym. Sci. A*, 1965, **3**, 181.
14. Young, R. H., Quirk, R. P. and Fetters, L. J., *Adv. Polym. Sci.*, 1984, **56**, 1.
15. Aranguren, M. I. and Macosko, C. W., *Macromolecules*, 1988, **21**, 2484.
16. Ferry, J. D., *Viscoelastic Properties of Polymers*. Wiley, New York, 1980.
17. Macosko, C. W. and Miller, D. R., *Macromolecules*, 1976, **9**, 199.
18. Miller, D. R., Vallés, E. M. and Macosko, C. W., *Polym. Eng. and Sci.*, 1979, **19**, 272.
19. Miller, D. R. and Macosko, C. W., *J. Polym. Sci. B*, 1987, **25**, 2441.
20. Miller, D. R. and Macosko, C. W., *J. Polym. Sci. B*, 1988, **26**, 1.
21. Di Nezio, M. S., M.Sc. thesis, Universidad Nacional del Sur, Argentina, 1996.
22. Gordon, M. and Scantlebury, G. R., *J. Chem. Soc. B*, 1967, **1**.
23. Sarmoria, C., Vallés, E. M. and Miller, D. R., *Macromolecules*, 1990, **23**, 580.
24. Stanford, J. L., Stepto, R. F. T. and Waywell, D. R., *J. C. S. Faraday I*, 1975, **71**, 1308.
25. Stepto, R. F. T., in *Developments in Polymerization—3*, ed. R. N. Haward. Applied Science Publishers, Barking, 1983, Ch. 3, pp. 81–141.
26. Dušek, K., Gordon, M. and Ross-Murphy, S. B., *Macromolecules*, 1978, **11**, 236.
27. Flory, P. J., *Principles of Polymer Chemistry*. Cornell University Press, Ithaca, NY, 1953.
28. Ilavský, M. and Dušek, K., *Macromolecules*, 1986, **19**, 2139.
29. Fasina, A. B. and Stepto, R. F. T., *Makromol. Chem.*, 1981, **182**, 2479.